  Bull. Chem. Soc. Jpn., 62, 2267—2272 (1989)

Preparation, Crystal Structure, and Solid State Properties of Highly Conductive (Phthalocyaninato)platinum Radical Salts: $PtPc(ClO_4)_{0.5}$ and $PtPc(AsF_6)_x$

Hideo YAMAKADO, Kyuya YAKUSHI,*,† Nobuhiro KOSUGI, Haruo KURODA,
Atsushi KAWAMOTO,†† Jiro TANAKA,†† Tadashi SUGANO,†††
Minoru KINOSHITA,††† and Shojun HINO††††
Department of Chemistry, Faculty of Science, The University of Tokyo, Hongo, Tokyo 113
††Department of Chemistry, Faculty of Science, Nagoya University, Furo-cho, Chikusa-ku, Nagoya 464
†††Institute for Solid State Physics, The University of Tokyo, Roppongi, Tokyo 106
††††Department of Image Science and Technology, Faculty of Engineering,
Chiba University, Yayoi-cho, Chiba 260
(Received January 20, 1989)

New conducting salts of (phthalocyaninato)platinum (PtPc), $PtPc(ClO_4)_{0.5}$ and $PtPc(AsF_6)_x$, were prepared by electrochemical oxidation. A crystal of $PtPc(ClO_4)_{0.5}$ belongs to a tetragonal system with a space group of *P4/mcc*, the lattice constants being a=14.062(1) Å, c=6.510(1) Å, and Z=2. They are metallic at least down to 120 K, the room-temperature conductivity being $\sigma=10^2$—10^3 S cm^{-1}. XPS indicates that the conduction pathway is located mainly at the ligand chain due to a partial oxidation of the ligand-centered HOMO. ESR experiments have also strongly supported this conclusion. The bandwidth of the ligand-centered conduction band has been estimated to be 1.2 eV from the plasma frequency, $\hbar\omega_p$=0.87 eV, which is obtained by the polarized reflectance spectrum.

Highly conductive iodine salts of metallo-macrocyclic compounds have been extensively studied by groups at Northwestern University.[1-10] These partially oxidized phthalocyanine salts have a stable metallic ground state against Peierls distortion at low temperature, although they have a one-dimensional column structure with a metal-over-metal overlapping mode. On the other hand, the mixed-valent platinum complex, $K_2Pt(CN)_4Br_{1/3}\cdot 3H_2O$ (KCP), has been reported to have a mixed-valent groud state between Pt^{2+} and Pt^{4+},[11,12] which might give rise to a movement of paired electrons.[13] However, it shows a semiconductive behavior at low temperature,[14] because it suffers the Peierls distortion.[15] Therefore it may be interesting to make a partially oxidized platinum chain which is stable against this type distortion. Such materials might possibly be found by searching for the conductive platinum macrocyclic compounds. This was the motivation of the present research. In this paper we report on the preparation and solid-state properties of the partially oxidized salts of (phthalocyaninato)-platinum (PtPc), $PtPc(ClO_4)_{0.5}$ and $PtPc(AsF_6)_x$, which were prepared for the first time in the research described here.

Experimental

PtPc was synthesized from phthalonitrile and $PtCl_2$,[16] and purified several times by a vacuum sublimation. The partially oxidized salts, $PtPc(ClO_4)_{0.5}$ and $PtPc(AsF_6)_x$, were obtained by the electrochemical method in a 1-chloronaphthalene solution using supporting electrolytes of $(n\text{-}Bu)_4NX$, (X=ClO_4 and AsF_6). The electrochemical reaction was carried out for about 2 weeks in a galvanostatic mode (1—5 μA) at 120 °C in an Ar or N_2 atmosphere. The concentration of PtPc was ca. 3×10^{-4} mol l^{-1}, and those of the supporting electrolytes were (2×10^{-3}—2×10^{-2}) mol l^{-1}. The crystals were grown along the c-axis, the typical dimensions being 0.01×0.01×2 mm^3. The chemical composition of $PtPc(ClO_4)_{0.5}$ was determined from an X-ray crystal structure analysis.

The intensities of X-ray diffraction were measured at room temperature with a Rigaku AFC-5 automated diffractometer combined with a Rotaflex RU-200, using Cu $K\alpha$ radiation monochromated with a graphite plate. The dimensions of the crystal used in this experiment were 0.03×0.03×0.6 mm^3. The crystal belongs to a tetragonal system with a space group of *P4/mcc*, the cell constants being a=14.062(1) Å, c=6.510(1) Å, and Z=2. We obtained 554 unique reflections, in which 405 reflections with $F_o>3\sigma(F_o)$ were used for the analysis. An absorption correction was made with a program (ACACA) written by C. T. Prewitt. The structure was solved by a heavy-atom method and was refined by a block-diagonal least-squares method with anisotropic temperature factors. The hydrogen atoms were neglected in this analysis. The final R-value was 0.055. The anisotropic temperature factors and F_o-F_c data are deposited as Document No. 8883 at the office of the Editor of Bull. Chem. Soc. Jpn. The computer program used in this analysis was UNICS III system.[17]

The electrical conductivity of a single crystal was measured along the needle axis from 290 K down to 10 K by the use of a four-probe ac method with a frequency of 70 Hz, the constant current being 10 μA. The voltage drop between the inner probes was detected by a lock-in-amplifier (EG & G 5205) which was controlled by a microcomputer. The phase change of the voltage was automatically checked at each temperature. Needle-like crystals were mounted on 10 μm gold wires with carbon paint to obtain electrical contact. The unnested voltage was tolerably small.

XPS was measured by a Kratos XSAM 800 ultrahigh vacuum photoelectron spectrometer using the Mg $K\alpha$ line as

† Present address: Institute for Molecular Science, Myodaiji-cho, Okazaki, Aichi 444.

the excitation source. PtPc was deposited on the copper sample holder through vacuum sublimation. Powdered samples of $PtPc(ClO_4)_{0.5}$ and $PtPc(AsF_6)_x$ were pressed onto the copper holder. No surface treatment was conducted so as to avoid any damage to the sample. Calibration of the spectrometer was performed by Au4f lines and the Au Fermi edge.

The ESR spectra were measured with a JEOL JES-FE1XG and a Varian E-112 using an X-band at temperatures between 290 and 4.2 K. About 80 slim crystals were aligned with silicone grease on a teflon sample holder so that the needle axes were parallel to each other. The crystals were so small that the ambiguity of the alignment was about 10°. The g-value was determined by a comparison of the ESR signal of solid Li-TCNQ. The spin susceptibility was calibrated by the integrated intensity of violanthrone, the static magnetic susceptibility of which had been measured. The intensity was obtained from a double integration of the ESR signal.

Polarized reflectance spectra were measured in the spectral range from 4200 to 25000 cm^{-1} with the polarization directions parallel and perpendicular to the *c*-axis at room temperature. The reflectance spectra were measured with a microspectrophotometer. The absolute reflectivity was obtained by comparing with the reflected light from a Si single crystal.

Results and Discussion

Crystal Structure. The atomic parameters of $PtPc(ClO_4)_{0.5}$ are compiled in Table 1. Figure 1 shows side and top views of the molecular column of PtPc in the crystal of $PtPc(ClO_4)_{0.5}$. The space group is the same as those of NiPcI,[1] $NiPc(BF_4)_{0.33}$,[7] $NiPc(ClO_4)_{0.42}$,[9] H_2PcI,[8] CoPcI,[6] and CuPcI.[10] The crystal is composed of molecular columns piled up along the *c*-axis. In this column the phthalocyanine molecules are stacked with a staggered angle of 40.7°. At the same time, the phthalocyanine molecules make molecular layers on the (001) plane. ClO_4^- is located at the interlayer position, as shown in the side view. The site occupancy of ClO_4^- is 0.5, so that the anions are positionally disordered. Since the diameter of ClO_4^- (ca. 5.6 Å)[19] is larger than half the *c*-axis, the anions and voids should be located alternately along the *c*-axis, and these one-dimensionally ordered anions are probably arranged randomly along the *a*- and *b*-axes. Furthermore, the large temperature factors of ClO_4^- indicate that the anion is also rotationally disordered. Table 2 shows a comparison of the average bond distances of PtPc. Since the atomic scattering factor of a platinum atom is much larger than those of carbon and nitrogen atoms, the standard deviations of the bond distances are large: 0.02 Å for Pt–N distance and 0.03—0.04 Å for N–C and C–C bond. In addition, the molecular geometry of the Pc ring is insensitive to the valency.[20] Therefore it is not possible to judge from the molecular geometry whether the ring is oxidized or not. Since the oscillation and Weissenberg photographs of $PtPc(AsF_6)_x$ are essentially the same as those of $PtPc(ClO_4)_{0.5}$, we consider that the former is isostructural to the latter.

Table 1. Fractional Atomic Coordinates (×10⁴) and Equivalent Temperature Factors ($B_{eq}=(4/3)\sum_{ij}\beta_{ij}(a_i\cdot a_j)$)

Atom	*x*	*y*	*z*	B_{eq}
Pt	0	0	0	2.9
N(1)	1296(16)	577(13)	0	4.2
N(2)	809(14)	2257(13)	0	3.7
C(1)	1475(22)	1530(22)	0	3.9
C(2)	2453(18)	1728(19)	0	4.1
C(3)	3028(18)	2569(17)	0	4.6
C(4)	4016(21)	2407(22)	0	6.3
C(5)	4445(20)	1507(23)	0	6.6
C(6)	3899(20)	675(23)	0	6.0
C(7)	2874(16)	807(18)	0	3.8
C(8)	2129(15)	131(22)	0	3.1
Cl	5000	5000	2500	17.2
O	4279(69)	4537(66)	1835(241)	18.2

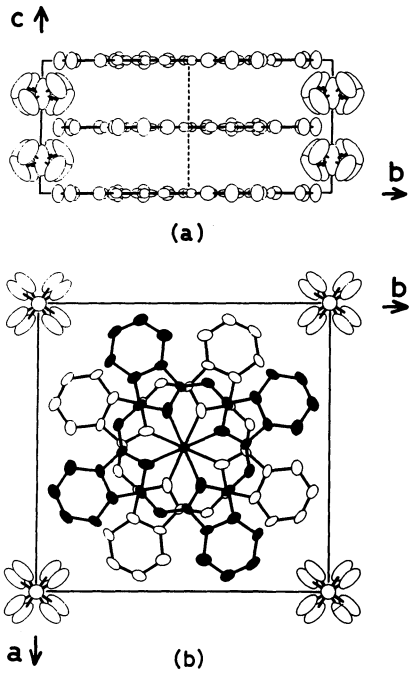

Fig. 1. (a) Side view and (b) top view of the crystal structure of $PtPc(ClO_4)_{0.5}$. The occupancy of ClO_4^- is 0.5.

Table 2. Average Bond Distances of PtPc

	$PtPc(ClO_4)_{0.5}$[a]	α-PtPc[b]	γ-PtPc[b]
$Pt-N_p$	1.99(2)	1.98	1.99
N_p-C_a	1.35(4)	1.38	1.40
N_m-C_a	1.36(4)	1.33	1.34
C_a-C_b	1.41(4)	1.49	1.44
C_b-C_b	1.42(4)	1.37	1.47
C_d-C_d	1.40(4)	1.40	1.38
C_b-C_c	1.44(4)	1.41	1.42
C_c-C_d	1.41(4)	1.41	1.42

a) This work. b) C. J. Brown.[18]

Electrical Resistivity. The electrical resistivity of $PtPc(ClO_4)_{0.5}$ along the *c*-axis is 10^{-2}—$10^{-3}\,\Omega$ cm at room temperature. The temperature dependence of the resistivity shown in Fig. 2 is one of the examples in which the cooling and warming rate is 0.5 K min^{-1}. The resistivity decreases at least down to 120 K upon cooling the sample. Below 100 K resistivity jumps take place at various temperatures which are not reproducible; the resistivity gradually increases up to 10^3 times the room-temperature value at 10 K. However, the resistivity recovers the starting value again upon warming the sample to room temperature. This temperature dependence of the resistivity is not reproducible against the heat cycles. The resistivity curve below 50 K cannot be described by a simple exponential function, $\rho(T)/\rho_{RT} \propto \exp(E_a/kT)$, but is well reproduced by the fluctuation-induced tunneling conduction model[21] which is applied to the analysis of the resistivity curves of doped polyacetylene and other inhomogeneous materials. We surmise that the metallic domains still remains at low temperature in $PtPc(ClO_4)_{0.5}$. A more elaborate investigation is necessary for an elucidation of the resistivity in the low-temperature region. Similar electrical properties have also been observed for $PtPc(AsF_6)_x$.

X-Ray Photoelectron Spectra. The X-ray photoelectron spectrum (XPS) has been used to determine the valency of atoms and molecules. For example, XPS played a crucial role in elucidating the mixed-valent state between Pt^{2+} and Pt^{4+} in the KCP crystal.[12] In the present case, however, no difference has been observed among PtPc, $PtPc(ClO_4)_{0.5}$, and $PtPc(AsF_6)_x$ as concerns the line shapes of $Pt4f_{7/2}$ and $Pt4f_{5/2}$, except for a slight increase (0.2 eV) in the linewidth for the oxidized salts. Their binding energies are the same as each other, the values being 73.2 and 76.6 eV for $Pt4f_{7/2}$ and $Pt4f_{5/2}$, respectively. As for the phthalocyanine ring, the line shape of the N1s spectrum is almost exactly the same as each other, and its binding energy is 398.9 eV. In contrast, the line shape of the C1s photoelectron spectra of $PtPc(ClO_4)_{0.5}$ and $PtPc(AsF_6)_x$ is slightly different from that of PtPc. Figure 3 shows a comparison of the line shapes of $PtPc(ClO_4)_{0.5}$ and PtPc. According to the theoretical work of NiPc by Kutzler and Ellis,[22] the highest occupied molecular orbital (HOMO) of NiPc is composed of the $2p_z$ orbitals of carbon atoms and has nodes at the nitrogen atoms and the nickel atom. Since this character of HOMO is also expected in PtPc, the observed result indicates that a partial oxidization occurs mainly in the phthalocyanine ring. The slight chemical shift of the binding energy of C1s is consistent with the ligand-centered oxidation. These XPS results mean that the conduction pathway is not on the Pt chain but, rather, on the Pc rings in contrast to KCP.

Electron Spin Resonance. Figure 4 shows the

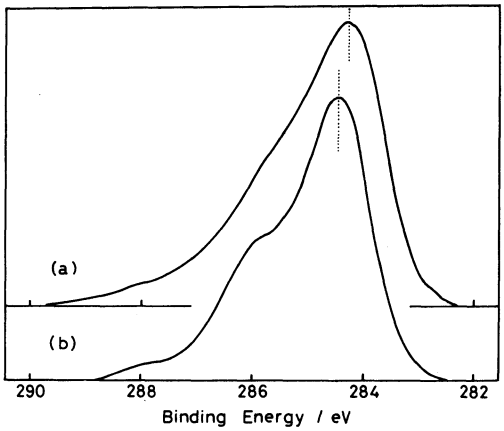

Fig. 3. XPS spectra of the C 1s region of (a) $PtPc(ClO_4)_{0.5}$ and (b) PtPc.

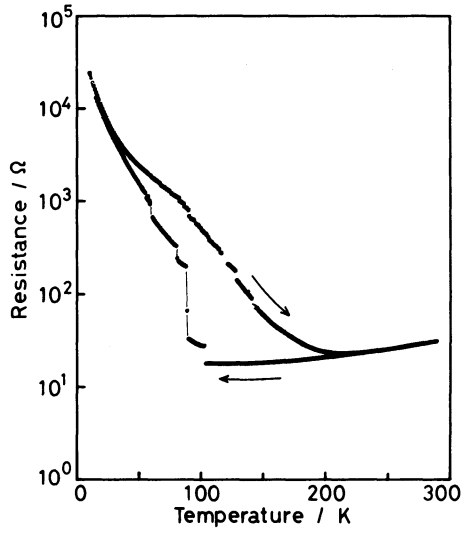

Fig. 2. The first heat cycle of the electrical resistivity of $PtPc(ClO_4)_{0.5}$.

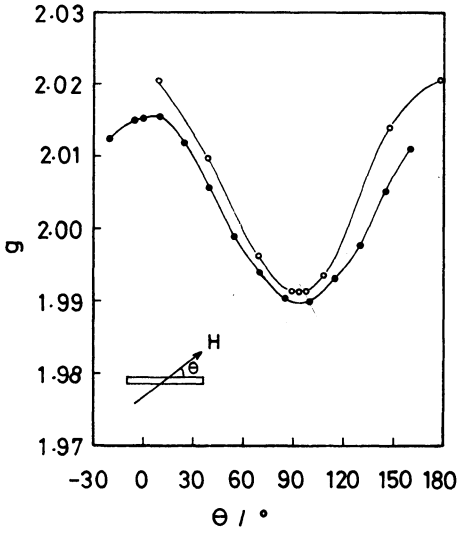

Fig. 4. Angular dependence of the ESR signal of $PtPc(ClO_4)_{0.5}$. The solid and open circles correspond to the room temperature and 4.2 K, respectively.

angular dependence of the g-value of $PtPc(ClO_4)_{0.5}$ at room temperature and 4.2 K. From the tetragonal symmetry of the crystal and molecule, the principal values of the PtPc molecule can be directly determined from this angular dependence. The principal values are given in Table 3, together with the corresponding values of the other related molecules. The symbols, // and ⊥, denote the directions parallel and perpendicular to the normal of the molecular plane. Since the principal values of $PtPc(ClO_4)_{0.5}$ are completely different from the corresponding values of KCP,[23] the unpaired electrons are not in the $5d_{z^2}$ band located at the platinum chain. On the other hand, the g-values are also slightly different from those of the ligand-oxidized cation radical, e.g. $Ni^{2+}Pc^{1-}$.[26] Therefore, the oxidation is mainly ligand-centered, though the unpaired electron also has a slight d-character. This result is similar to that of $NiPc(SbF_6)_{0.5}$.[24,25] However, the relation, $g_{//} > g_{\perp}$, is reverse to that of $NiPc(SbF_6)_{0.5}$,[24,25] in which the d-character of the unpaired electron is interpreted based on the exchange interaction between the conduction electrons on the ligand and the small amount of the localized spins on the $3d_{z^2}$ orbital of nickel atoms. This anisotropy indicates that the $5d_{z^2}$ orbital of Pt is not responsible for the d-character of the unpaired electron, but that the orbital of the unpaired electron has a character of d_{xz} and d_{yz}.[27] It is not reasonable to simply replace the role of $5d_{z^2}$ by $5d_{xz}$ and $5d_{yz}$, because the latters are expected to be strongly hybridized with the π-orbital (e_g) of the ligand in contrast to the former.[22] We thus consider that this molecular orbital with e_g symmetry is mixed to some extent with the ligand-centered HOMO (a_{1u}) in the solid state because the symmetry restriction is released in the general point of the Brillouin zone. However, the contribution of the e_g orbital seems to be very small, because the observed g-value is close to that of the ligand-centered unpaired spin, even at low temperature (as described in the next section). This conjecture is supported by the experimental result of XPS that the oxidation occurs mainly at the ligand part. The different anisotropy of the g-value between PtPc and NiPc is attributed to the electronic structures of their molecules. Unfortunately, details of the electronic structure of PtPc are not known, as compared with that of NiPc.

Figure 5 shows the temperature dependences of the spin susceptibilities, linewidths, and g-values. Upon cooling, $g_{//}$ and $g_{\perp}$ slightly increase from 2.016 and 1.989 to 2.023 and 1.992 at 4.2 K, respectively. This temperature dependence is much weaker than that of $NiPc(SbF_6)_{0.5}$.[25] This slight increase probably sug-

Table 3. Principal g-Values of $PtPc(ClO_4)_{0.5}$ and Other Complexes at Room Temperature

Compound	$g_{//}$	$g_{\perp}$	Reference
$PtPc(ClO_4)_{0.5}$	2.016	1.989	This work
$PtPc(AsF_6)_x$	2.016	1.990	This work
$Pt(CN)_4Br_{1/3}\ 3H_2O$	1.946	2.336	Mehran and Scott[23]
$NiPc(SbF_6)_{0.5}$	1.994	2.030	Yakushi et al.[24,25]
$Ni^{2+}Pc^{1-}$	2.003	2.003	Bobrovskii and Sidorov[26]

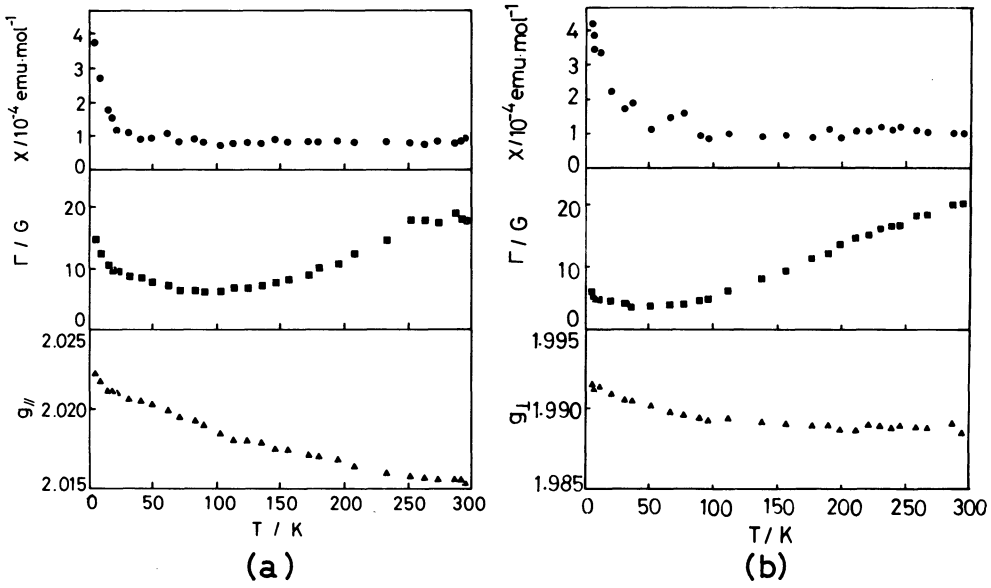

Fig. 5. Temperature dependence of the spin susceptibilities (χ), linewidths (Γ), and g-values (g). (a) $H//c$ and (b) $H \perp c$.

gests a change in the degree of mixing between the e_g and a_{1u} bands. The line shape of the ESR signal is Lorentzian over the whole temperature range. The spin susceptibility, which is obtained by the double integration of the observed signal, remains almost constant down to ca. 20 K. Combining this result with the metallic behavior of the electrical resistivity, the temperature-independent spin susceptibility is attributable to Pauli paramagnetism. The linewidths of organic metals usually decrease upon lowering the temperature, since they are determined mainly by the spin relaxation through the so-called Elliot mechanism.[28] Thus the gradual decrease of the linewidth also supports the view that the origin of the unpaired electrons is conduction electrons. This magnetic result suggests that $PtPc(ClO_4)_{0.5}$ is metallic, at least down to 20 K. Assuming the one-dimensional tight-binding model, we estimated the bandwidth, $4t$, using

$$4t = 4N_A\mu_B^2/(\pi \sin(k_fc)\chi), \quad (1)$$

where N_A is the Avogadro constant, μ_B the Bohr mageton, k_f the Fermi wave vector, c the inter-planar distance between the adjacent PtPc molecules, and χ the spin susceptibility (measured with a unit of emu mol^{-1}). The bandwidth of the ligand-centered band has been estimated to be 0.6—0.8 eV using $\chi=(1.0—0.7)\times10^{-4}$ emu mol^{-1} and $k_fc=(3/4)\pi$. The rise-up of χ in the region of $T<20$ K is attributable to the localized spins, the concentration of which is 4×10^{-3} spins per one $PtPc(ClO_4)_{0.5}$. Since the angular dependence of the g-value of the localized spins is almost the same as that of the conduction electrons (as shown in Fig. 4), the origin of the localized spins is not the magnetic impurity but, rather, a crystal defect. Incidentally, the ESR spectrum of $PtPc(AsF_6)_x$ is essentially the same as that of $PtPc(ClO_4)_{0.5}$, including the temperature dependence.

Polarized Reflectance Spectra. Figure 6 shows the reflectance spectra of $PtPc(ClO_4)_{0.5}$ polarized parallel and perpendicular to the c-axis. The plasma-edge like dispersion is observed only in the $//c$ polarization. This strong anisotropy clearly indicates the presence of a one-dimensional conduction band along the c-axis. We analyzed the $//c$ spectrum based on the Drude model, and obtained the plasma frequency, $\omega_p=7010$ cm^{-1}, the relaxation time of the conduction electrons, $\tau=0.8\times10^{-14}$ s, and the dielectric constant contributed from the electronic excitations in the higher wave number region, $\varepsilon(\text{core})=2.31$. The reflection spectrum calculated from these parameters is drawn by solid lines in Fig. 6. The bandwidth, $4t$, was calculated on the assumption of the one-dimensional tight-binding model using

$$4t = \{V_m(\hbar\omega_p)^2\}/\{4e^2c^2\sin(k_fc)\}, \quad (2)$$

where V_m is the volume of $PtPc(ClO_4)_{0.5}$, e the unit charge of an electron, and k_f and c are the same as those defined in Eq. 1. The bandwidth was estimated to be 1.2 eV, using $V_m=6.437\times10^{-22}$ cm^3, $\hbar\omega_p=0.87$ eV, and $k_fc=(3/4)\pi$. This bandwidth is 1.5—2.0 times larger than that estimated from the spin susceptibility. The difference between them is attributable to the effect of the electron-electron Coulomb interaction.[29] Since the optical spectrum of $PtPc(AsF_6)_x$ is the same as $PtPc(ClO_4)_{0.5}$, we surmise $x\approx0.5$ in $PtPc(AsF_6)_x$, because the position of the plasma edge in the reflection spectrum reflects the concentration of the conduction electrons, which is related to the chemical ratio.

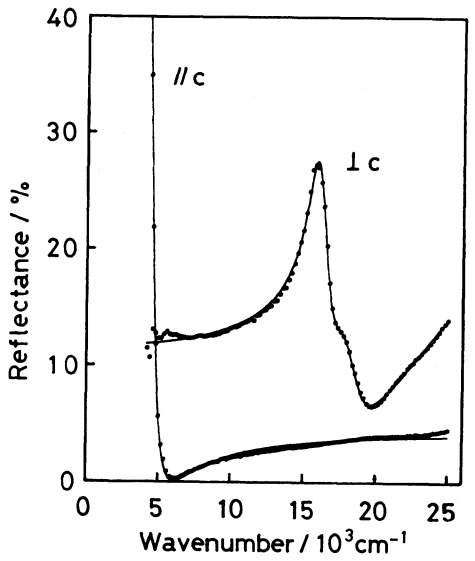

Fig. 6. Polarized reflectance spectrum of the $PtPc(ClO_4)_{0.5}$ single crystal. The circles and the solid lines are respectively the experimental data and the simulated curves based on the Drude model for the $//c$ spectrum and the Lorentz model for the $\perp c$ spectrum.

The $\perp c$ spectrum was simulated by three Lorentz oscillators so as to reproduce the experimental curve. The simulated curve is represented by the solid line in Fig. 6. The resonance frequencies of the Lorentz oscillators in the visible region are 16000 and 17900 cm^{-1}. The 16000 cm^{-1} electronic transition is assigned to the interband transition which corresponds to the Q-band in the free molecule of phthalocyanine. Probably, the shoulder at 17900 cm^{-1} cannot be assigned to the vibrational structure of the Q-band, since the intensity ratio to the main peak at 16000 cm^{-1} and the separation of the excitation energies depend significantly upon the central metals of such salts as $NiPc(SbF_6)_{0.5}$[25] and $CoPc(AsF_6)_x$.[30] The origin of this shoulder is not clear at present. However, it is possibly related to the mixed-valent nature of the phthalocyanine ring, since the monoclinic PbPc crystal[31] exhibits a strong Q-band, the shape of which is a single Lorentzian with a width of 1000 cm^{-1} (FWHM).[32]

We prepared $PtPc(ClO_4)_{0.5}$ and $PtPc(AsF_6)_x$, which were the first oxidized salts of PtPc, in the process of searching for a stable metallic platinum chain with a mixed-valent state. Both PtPc salts are isostructural and have one-dimensional column structures like the iodine complex of NiPc. They are metallic at least down to 120 K and probably to 20 K, or possibly to a temperature lower than that. Contrary to our expectation, however, the conducting pathway is not located on the platinum spine, but mainly on the ligand chain. The solid state properties are almost the same as those of $NiPc(SbF_6)_{0.5}$,[25] but the ESR properties are remarkably different.

References

1) C. J. Schramm, R. P. Scaringe, D. R. Stojakovic, B. M. Hoffman, J. A. Ibers, and T. J. Marks, *J. Am. Chem. Soc.*, **102**, 6702 (1980).

2) T. E. Phillips, R. D. Scaringe, B. M. Hoffman, and J. A. Ibers, *J. Am. Chem. Soc.*, **102**, 3435 (1980).

3) J. Martinsen, L. J. Pace, T. E. Phillips, B. M. Hoffman, and J. A. Ibers, *J. Am. Chem. Soc.*, **104**, 83 (1982).

4) J. Martinsen, S. M. Palmer, J. Tanaka, R. C. Greene, and B. M. Hoffman, *Phys. Rev. B*, **30**, 6269 (1984).

5) S. M. Palmer, J. L. Stanton, N. K. Jaggi, B. M. Hoffman, J. A. Ibers, and L. H. Schwartz, *Inorg. Chem.*, **24**, 2040 (1985).

6) J. Martinsen, J. L. Stanton, R. L. Greene, J. Tanaka, B. M. Hoffman, and J. A. Ibers, *J. Am. Chem. Soc.*, **107**, 6915 (1985).

7) T. Inabe, S. Nakamura, W. B. Liang, T. J. Marks, R. L. Burton, C. R. Kannewurf, and K. Imaeda, *J. Am. Chem. Soc.*, **107**, 7224 (1985).

8) T. Inabe, T. J. Marks, R. L. Burton, J. W. Lyding, W. J. McCarthy, C. R. Kannewurf, G. M. Reisner, and F. H. Herbstein, *Solid State Commun.*, **54**, 501 (1985).

9) M. Almeida, M. G. Kanatzidis, L. M. Tonge, T. J. Marks, H. O. Maracy, W. J. McCarthy, and C. R. Kannewurf, *Solid State Commun.*, **63**, 457 (1987).

10) M. Y. Ogawa, J. Martinsen, S. M. Palmer, J. L. Stanton, J. Tanaka, R. L. Greene, B. M. Hoffman, and J. A. Ibers, *J. Am. Chem. Soc.*, **109**, 1115 (1987).

11) K. B. Efetov and A. I. Larkin, *Sov. Phys. JETP*, **42**, 390 (1976).

12) G. A. Sawatzky and E. Antonides, *J. Phys.*, **37**, C4-117 (1976).

13) H. Nagasawa, *Phys. Status Solidi B*, **109**, 749 (1982).

14) A. S. Berenblyum, L. I. Buravov, M. D. Khidekel', I. F. Shchegolev, and E. B. Yakimov, *JETP Lett.*, **13**, 440 (1971).

15) J. Bernasconi, P. Bruesch, and H. R. Zeller, *J. Phys. Chem. Solids*, **35**, 145 (1974).

16) P. A. Barett, C. E. Dent, and R. P. Linstead, *J. Chem. Soc.*, **1936**, 1719.

17) T. Sakurai and K. Kobayashi, *Rep. Inst. Phys. Chem. Res.*, **55**, 69 (1979).

18) C. J. Brown, *J. Chem. Soc. A*, **1968**, 2494.

19) R. D. Shannon, *Acta Crystallogr., Sect. A*, **32**, 751 (1976).

20) K. Yakushi, M. Sakuda, H. Kuroda, A. Kawamoto, and J. Tanaka, *Chem. Lett.*, **1986**, 1161.

21) P. Sheng, *Phys. Rev. B*, **6**, 2180 (1980). This model explains well the resistivity curve from 50 K to 4.2 K which was measured on the different sample shown in Fig. 2.

22) F. W. Kutzler and D. E. Ellis, *J. Chem. Phys.*, **84**, 1033 (1986).

23) F. Mehran and B. A. Scott, *Phys. Rev. Lett.*, **31**, 1347 (1973).

24) K. Yakushi, H. Yamakado, M. Yoshitake, N. Kosugi, H. Kuroda, A. Kawamoto, J. Tanaka, T. Sugano, M. Kinoshita, and S. Hino, *Synth. Met.*, **28**, F95 (1989).

25) K. Yakushi, H. Yamakado, M. Yoshitake, N. Kosugi, H. Kuroda, T. Sugano, M. Kinoshita, A. Kawamoto, and J. Tanaka, *Bull. Chem. Soc. Jpn.*, **62**, 687 (1989).

26) A. P. Bobrovskii and A. N. Sidorov, *J. Struct. Chem. (Engl. Transl.)*, **17**, 50 (1976).

27) J. S. Griffith, *Discuss. Faraday Soc.*, **26**, 81 (1958).

28) R. J. Elliot, *Phys. Rev.*, **96**, 266 (1954).

29) C. S. Jacobsen, *J. Phys. C*, **19**, 5463 (1986).

30) H. Yamakado and K. Yakushi, unpublished data.

31) Since the first singlet excited state of metallo-phthalocyanine is degenerate, the Q-band is split into 4 absorption bands in almost all metallo-phthalocyanine crystals because of the low site symmetry and the exciton effect. However, the exceptional case is found in the monoclinic form of PbPc, in which the arrangement of PbPc is nearly tetragonal like the partially oxidized salts of metallo-phthalocyanine.

32) Y. Iyechika, K. Yakushi, and H. Kuroda, *Chem. Phys.*, **87**, 101 (1984).